SVU-International Journal of Engineering Sciences and Applications (2024) 5(2): 209-221
Print ISSN 2785-9967 | Online ISSN 2735-4571
DOI 10.21608/SVUSRC.2024.271195.1191

Modelling and Finite Element Analysis of Structural Modifications in Brake Pad and Disc to Suppress Squeal

Mohamed Essam[1,*], Abdelhameed A. Zayed[1], Fady Ibrahim[2], Ahmed M El-Kassas[1], and Ahmed Nabhan[3]

Abstract This paper deals with the problem of squeal noise in disc brakes, which is a major concern for researchers and brake manufacturers. The finite element method and complex eigenvalue analysis are used to explore how changing the shape of the disc and the pad affect the squeal noise. Six different pad shapes and two different disc vane shapes under three braking scenarios are compared and investigated. The numerical results indicated that appropriate structural modification of a disc brake system can lower the brake squeal to a certain degree. Moreover, the results demonstrate that curved disc vane could eliminate squeal and has more significant effect rather than pad shape. The curved disc vane showed a steady performance in all working conditions through eliminating all the unstable modes that were generated from the base model. Furthermore, the pad modifications were also able to remove the generated unstable modes from the base model however, they introduced other unstable modes with series tendency of instability and higher propensity to squeal.

Keywords: Brakes, Complex eigenvalue analysis, Squeal, FE, Tendency of instability

1 Introduction

One of the key factors that influence the vehicle market is the comfort of the vehicle. Noise vibration harshness (NVH) is one of the factors that lowers vehicle quality. Brake designers face a lot of difficulties because of NVH. The brake noise, vibration, harshness cause warranty costs of one billion dollars every year in North America [1]. The friction materials companies invest huge amount of money to deal with NVH problems for high performance [2]. J.D Power IQS (Initial Quality Study) survey shows that brake system complaints are the main vehicle quality issues, mostly because of NVH, making researchers work on NVH solutions. Brake squeal is a loud noise that happens when braking is applied. It is a serious problem for car makers, as it causes many customers to complain and ask for refunds. To make cars quieter and more comfortable, it is important to control brake noise and vibration. By getting rid of or lowering brake squeal, customer satisfaction can be increased, and warranty costs can be decreased [3], [4], [5]. Brake noise can be divided into many types depending on the frequency and the source of the sound [6] as Fig.1 shows. It can be seen that there a lot of types of brake noise including: judder, groan, moan, howl and squeal. squeal occurs due to several mechanisms, firstly decreasing of kinetic coefficient of friction (μ_k) with the sliding velocity (v_s) increasing [7], secondly sprag slap [8], thirdly Mode coupling [9] [10] and Hammering [11]. None of these mechanisms could explain the squeal phenomenon alone, although mode coupling is considered one of the most used theories used to explain the squeal occurrence. Mode coupling refers to the coupling of two or more modes of brake components of the brake system producing an optimum condition for squeal. So, So, to prevent this phenomenon from occurrence, geometrical modifications for various disc brake components especially brake pad and disc were introduced. The purpose of this modifications is to shift the natural frequency of the brake components to avoid the coupling of the close modes together. Investigation of disc brake squeal carried out through different methods to

Received: 16 March 2024/ Accepted: 23 June 2024
* Corresponding Author: Essam, Mohamed
moh.essam947@f-eng.tanta.edu.eg
1. Production Engineering and Mechanical Design Department, Faculty of Engineering, Tanta University, Tanta 31521, Egypt.
2. Automotive Engineering Department Faculty of Engineering Ain shams University, Cairo11517, Egypt.
3. Production engineering and Mechanical Design Depart. Faculty of Engineering, Minia University, El Minia 61111, Egypt.

characterize the phenomenon and study the effect of different parameters affecting brake squeal. Experimental methods could be used through dynamometer tests to study the different parameters that cause squeal and the solution. For eliminating this phenomenon, a vibration dynamometer Link 3900 with procedures of SAE J2521-2013 braking test standard used to evaluate the squeal behavior of laser machined discs [12]. The link between the change in the third-body layer and the occurrence of squeals in sliding dry contact was investigated through pin on disc (POD) test rig [13]. The effect of adding constrained layer material to the pads to provide damping for the system was studied experimentally. Unfortunately, the conducted experiments are expensive and time consuming, also results from these tests that are valid for a certain type of brake system or vehicle not necessarily valid for the others and don't provide an insight into the mechanism of squeal noise generation [14]. On the other hand, the analytical and numerical modelling can deal with different brake conditions and a wide variation of parameters, this way helped in the improvement of noise measurement in the design stage before building the prototype and provide guidance for the experimental setup.

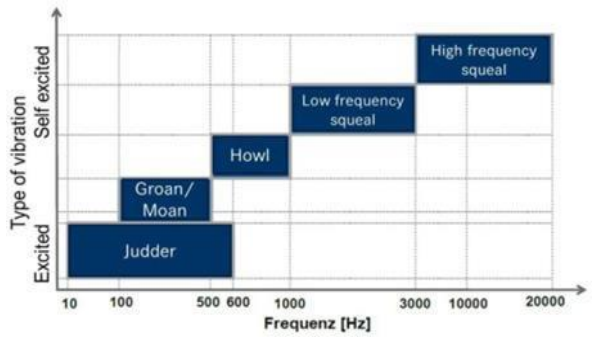

Fig. 1 Frequency range for Brake noise classification adopted from [6].

Numerical methods can be divided into two categories: lumped parameter models and finite element models. The first model, known as the lumped parameter model, has a limited number of degrees of freedom. These models have been extensively reviewed and are instrumental in understanding the mechanisms that cause brake squeal [15], [16], [17]. A unique dynamic brake system concept featuring a double-layer pad was introduced. The Stribeck friction model that is negative velocity gradient model was used to examine the impact of pad mass distribution and connection stiffness on the stability of the braking system and stick-slip vibration [18]. A2-DOF mass-spring-damper system, positioned on a moving belt, was created, with instability linked to both the Stribeck effect and the mode-coupling effect [19]. The primary objective of the study is to examine the impact of high frequency excitation (HFE) on the system's dynamics and stability. A dual-pin-on-disc setup was used to investigate friction-induced stick-slip vibration, and both experimental and theoretical analyses were conducted in [20]. The influence of tangential harmonic excitation on friction-induced vibration in multi-degree-of-freedom systems connected in the tangential and normal directions was explored using a simple two-degree-of-freedom system. A study investigates the five-degree-of-freedom mass-on-oscillating-belt model, focusing on three types of non-linearities: contact stiffness, non-smooth behavior, and geometrical non-linearity caused by the mass slider's load on the rigid belt, highlighting the importance of transient dynamic analysis in addressing friction-induced vibrations [21]. A dynamic model that considered the gyroscopic effect, negative friction slope, and mode coupling with non-proportional damping was developed examining the examining the effects of the pad's angular velocity, stiffness, damping coefficient, the friction coefficient, and the pad geometry (opening angle) on the optimization of disc brake parameters [22]. The Finite Element (FE) method has become a popular tool in recent years for studying disc brake squeal. It offers the flexibility to simulate any changes in disc brake components and any operating conditions. Two main strategies are employed to forecast squeal frequencies: firstly, Complex Eigen Value Analysis (CEA) in the frequency domain, and secondly, Transient Dynamic Analysis (TDA) in the time domain [23]. The outcomes from TDA can be transformed from the time domain to the frequency domain using Fast Fourier Transform. While CEA has been widely used, TDA is becoming increasingly popular in research [24], [25], [26], [27], [28]. The availability of various finite element software with high computational capabilities has provided researchers with the opportunity to simulate different geometric modifications to the disc brake components to mitigate the induced squeal [29]. This also includes the ability to conduct various parametric studies on the components' material properties or simulate different braking scenarios such as changing the braking pressure, velocity, temperature, and coefficient of friction. Investigations have been conducted into pad shape modification for high-frequency squeal suppression using straight chamfer, radial chamfer, diamond chamfer, and center slot [30]. On the other hand, disk asymmetry has been shown to reduce bending modes splitting by creating holes or attaching masses, thereby reducing squealing propensity [31]. A parametric study using Abaqus was carried out to assess system stability using a simplified model with pads and rotor [32]. The structural changes were investigated to disc brake rotors effect on squeal reduction using finite element model that is validated experimentally [33]. It suggested twelve rotor shape changes and their

performance was simulated via finite element that showed that the rotor hat asymmetry could eliminate all the un stable modes. Finite element analysis revealed curved rotor vanes and radial pad chamfer for best squeal suppression. along with lumped parameter model compared pad and rotor contact and showed that pad damping properties greatly influence disc brake system stability [34]. The influence of cross-drilled and slotted rotor patterns on automotive disc brake squeal was also studied. A link between mode frequencies and frictional surface patterns was found, which lead to squeal noise [35]. Modification in caliper design were applied to get uniform pressure distribution, which improved squeal reduction efficiency. The new design was simulated CEA and verified with bench test. The caliper design lowered noise occurrence from 19.27% to 3.63% [36]. Eliminated low frequency squeal by adding groove to hub of the rotor and modifying the thickness of tie bar of the carrier and the results were verified experimentally [37]. The compressive strain of a brake pad influence on brake noise examined and developed an optimized brake-pad scheme [38]. A dynamometer test checked the effectiveness of the optimized scheme and confirmed a clear reduction in brake noise. The compressive strain of a brake pad was changed using four methods: elastic modulus, section outlines, lining widths, and chamfers. The work done in [39] adapted the Taguchi technique to find the best disc vane shape and material for squeal elimination. The contacts behavior and noise of railway brakes were studied experimentally and numerically with finite element analysis and lumped parameter model [40].

Thise paper used CEA to study how brake pads and disc changes impact squeal likelihood. Six pad shape modifications and two-disc vane modifications are tested using CEA. A comparison is made at each working condition between the base model and the six pad shapes and also between the disc vane modifications via tendency of instability (TOI) parameter. A comprehensive comparison is also made between the proposed modifications based on the TOI. Thise paper highlights the vital role of geometrical modifications of the disc brake system components specially the pad and the disc in squeal suppression and instability decrement. The rest of this paper as structured as follows. Section 2 introduces the computational model complex eigenvalues analysis and the finite element model. The results with their discussions are presented in Section 3 while Section 4 summarizes the concluding remarks.

2. Approach and Computational Model

2.1 Analysis of Complex Eigenvalues

In this section the principle of CEA is described. During the braking process, the frictional interaction between the brake pad and the disc can trigger a dynamic imbalance within the system. This imbalance can generate noise, often referred to as squeal.

To investigate the potential occurrence of disc brake squeal, a stability examination is conducted and the unstable patterns are associated with potential squeal events. The system is governed by the following equation [38]:

$$M\ddot{x}+C\dot{x}+Kx = F \tag{1}$$

Where M, C, and K are the system's mass, damping, and stiffness matrices respectively and x, $\dot{x}$, $\ddot{x}$ are the displacement, velocity and acceleration vectors. In the brake system, the friction force at disc brake interface mainly contribute to the variable force function which is expressed as

$$F= \mu K_f .x \tag{2}$$

where μ is the coefficient of friction between the lining material and the disc and K_f is the friction stiffness matrix. Combining equation (1) and (2) will give us:

$$M\ddot{x}+C\dot{x}+(K-\mu K_f)x = 0 \tag{3}$$

Now due to the friction force the system stiffness is coupled and the stiffness matrix is asymmetric matrix which leads to the asymmetry of the characteristic matrix. So, for the underdamped system, the eigen values come in the form of complex conjugate pairs so the characteristic equation is:

$$\det\left(\lambda^2 M+\lambda C+K-\mu K_f\right) = 0 \tag{4}$$

$$\lambda_{i1,2} = \sigma_i \pm j\,\omega_i \tag{5}$$

Where ω is the circular frequency in rad/sec of the mode and σ is the real part of mode. indicates the instability of the mode, in other words, if σ is positive, the mode is unstable and if σ has negative value, the mode is stable. The corresponding damping ratio to the mode is given as

$$\text{Damping ratio} = \frac{-2\times\sigma}{\omega} \tag{6}$$

Yang et al [41] resolved squeal problem at 1800 Hz and considered a critical value of the damping ratio equals to -0.01 which means that value less than this value points to the instability of the mode and above this value means that the mode tends to be more stable, by presenting shape modifications for pad lining, rotor and caliper. These changes were effective in reducing the squeal existence. To make an analysis and comparison between the proposed modifications the tendency of instability (TOI) will calculated for each modification for the given working conditions through the following equation

$$\sum_i \frac{\sigma_i}{\omega_i}\times 1000, \quad \sigma_i>0 \tag{7}$$

This parameter has been used by many researchers [42],[43],[44] to assess the performance of various structural modifications of the brake system.

2.2. Finite Element Model of the Disc Brake

Abaqus software is used to perform the Complex Eigen Value Analysis (CEA) and, in the order to that, there are four steps that must be followed:

1. Nonlinear static analysis in which the pressure is applied in the first step.
2. Nonlinear static analysis in which rotational motion is applied to the rotor in the second step.
3. Natural frequency extraction in the third step.
4. Complex frequency extraction in the fourth step.

It is mentioned in [45] that squeal is divided into low squeal frequency squeal occurs between 1-5 kHz and high frequency squeal above 5 kHz. Consequently, the CEA analysis is preformed between 1000 Hz and 13000 Hz. The model used in this study is the full disc brake model shown in Fig.2. The material properties of the components and the type of element used in meshing of every part are listed in Table 1. Figure 3 shows the shape of the elements used in this study. In this analysis, three working conditions with different pressure and coefficient of friction, and fixed velocity is employed as indicated in Table 2. The modifications of the pad are indicated in Fig.4 and the dimensions of the geometrical modifications applied to the pads are in Fig.5. knowing that the slot and chamfer dimensions are fixed in all modifications. Figure 6 indicates the disc modifications. The description of the different models and its labels are displayed in Table 3. It's important to emphasize that all pad modifications were used with the base model disc vane shape, while all the modified disc vanes were used with the base model pad shape.

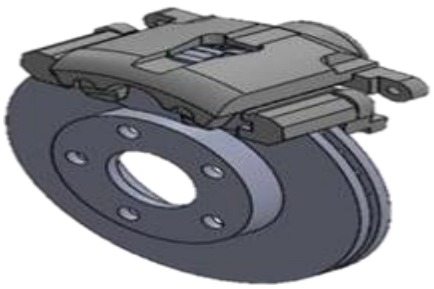

Fig. 2 The disc brake model used in the analysis.

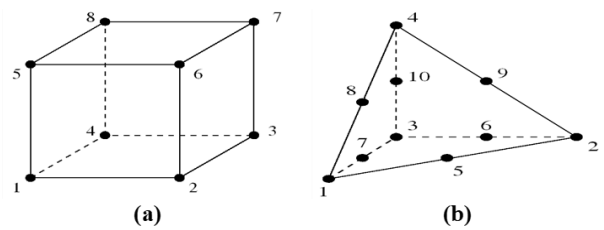

Fig. 3 The shape of the element type used (a) hexahedral element(C3D8) (b) tetrahedron element(C3D10).

Table 1 Material properties of disc brake parts

Part	Density (kg/m^3)	Young's modulus [MPa]	Poisson's ratio	Element Type
Disc	6257	135000	0.3	C3D8
Caliper	6533.6	170000	0.3	C3D10
Carrier	6094	155000	0.3	C3D10
Backplate	6836.92	259000	0.3	C3D8
Friction material	1767.44	9000	0.3	C3D8
Piston	7121	260000	0.3	C3D8
Metal clip	9548.5	190000	0.3	C3D8

Table 2 The working conditions (WC) used in the analysis.

Working Condition	Symbol	Pressure [MPa]	Friction Coefficient	Velocity [rad/sec]
1	WC1	1	0.45	
2	WC2	1.5	0.55	5
3	WC3	2	0.65	

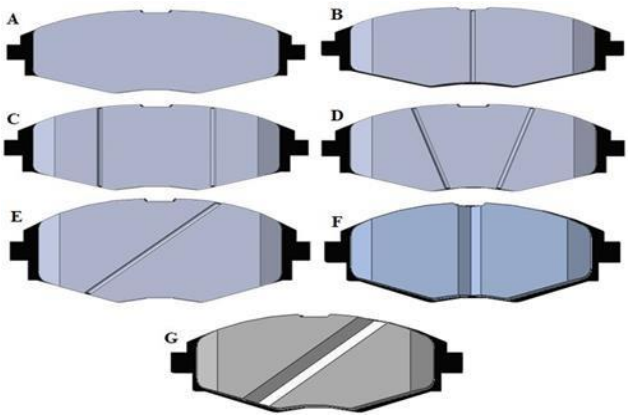

Fig. 4 The modified pad shapes (a) BM, (b)PM1, (c)PM2, (d)PM3, (e)PM4, (f)PM5, and (g)PM6.

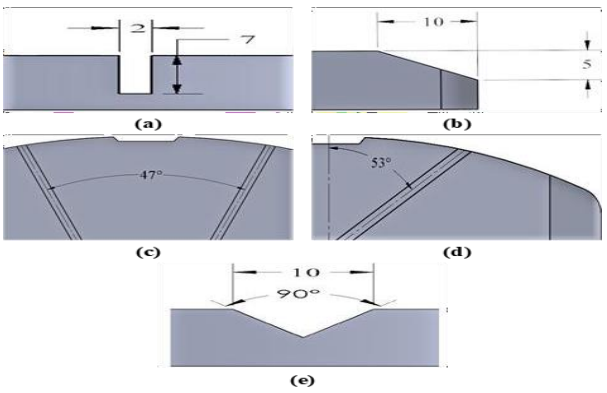

Fig. 5 Dimensions of different geometrical modifications in [mm] (a) slot dimensions (b) chamfer dimensions (c) angle between slots in PM3 (d) inclination angle in PM4 and PM6 (e) V slot dimensions

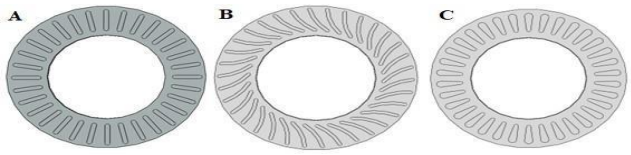

Fig. 6 the shape of disc vane (a) BM, (b) DM1, and (c)DM2

Table 3 The modifications made for both pad and disc and their description**.**

Parts	Name	Label	Description
Pad	Base model	BM	No modifications in the pad or the disc
	1st Modification	PM1	Straight chamfers from both sides with central slot.
	2nd Modification	PM2	Straight chamfers from both sides with two parallel slots 47 apart.
	3rd Modification	PM3	Straight chamfers from both sides with triangular slots
	4th Modification	PM4	Straight chamfers from both sides with one diagonal slot
	5th Modification	PM5	Straight chamfers from both sides with central V shaped slot
	6th Modification	PM6	Straight chamfers from both sides with one V shaped diagonal slot
Disc	1st Modification	DM1	The disc has curved vanes
	2nd Modification	DM2	The disc has Tapered vanes

3. Results and Discussion

In this study CEA is preformed up to 13 kHz in which squeal is predicted to take place. The effect of varying the coefficient of friction and the braking pressure with constant rotating speed is explored. Firstly, the base model is studied and the unstable modes are evaluated at the diversified working conditions given in Table 2. Secondly, the system with modifications in the pad shape and rotor vane shape are investigated. Finally, the behaviors of these changes are compared with the base model for the same working conditions by calculating the tendency of instability (TOI) for each configuration at given working conditions.

3.1. Complex Eigenvalue Analysis (CEA) of the base model

Figure 7 presents the unstable modes of the base model at the three working conditions and Fig.8 shows the shape of unstable modes of the base model in the first working condition. It can be seen that the base model in any working conditions produces in the given operating conditions unstable modes all lie in the high frequency region above 5 KHz which gives an indication that this model has the same behavior as model used by [34] as displayed in Fig.9 as it generated six squeal modes four of them in the high frequency squeal region. The blank shape of pad and straight vanes tend together to give high frequency squeal as studied where there complex eigen value analysis predicated five frequencies one only in the low frequency region while the other ones where in high frequency region [46].

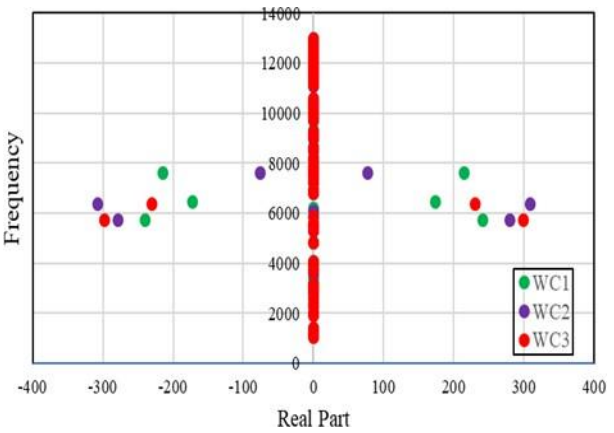

Fig. 7 The unstable modes generated from the base model in the three working conditions**.**

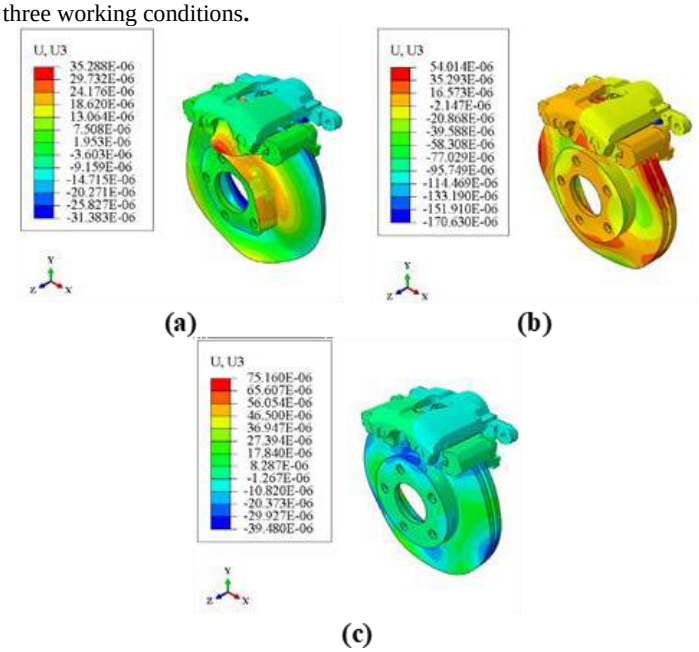

Fig. 8 The unstable modes of the base model in the first working condition (a) mode19 (b) mode 23 (c) mode29.

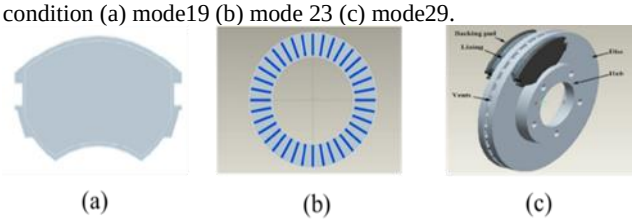

Fig. 9 The base model used by [34] (a) brake pad shape (b) disc vane shape (c) the shape of mode

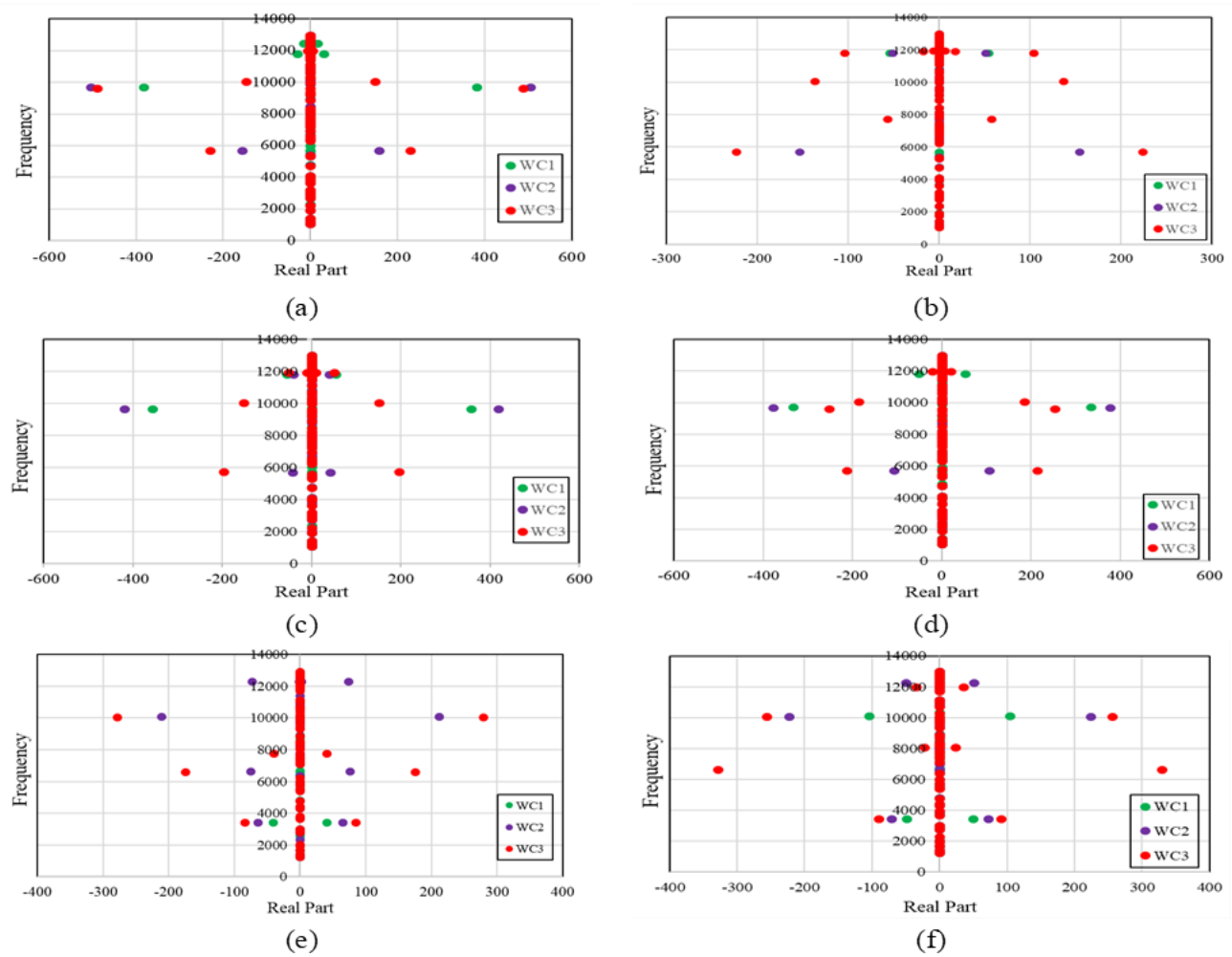

Fig.10 The individual performance of each pad modification at the three given conditions (a)PM1 (b)PM2 (c)PM3 (d)PM4 (e)PM5 (f)PM6.

3.2 Performance comparison in the different working conditions

3.2.1 Pad Modification

In this section an assessment for the proposed modifications of pad shape is done at the given three working conditions. Figure 10 shows the behavior of each pad modification individually at the given conditions.

3.2.1.1 First working condition

In the first working condition the applied pressure was 1 MPa and the coefficient of friction was 0.45. Figure 11 shows the unstable modes in each modification along with base model and the resulted values are emphasized in Table 4. In this operating state, all proposed modifications are able to eliminate the unstable modes of the base model. Most of the generated modes by the pad shapes lies in high frequency squeal region except for PM5 and PM6 that have two modes in low frequency region. The modes, in high frequency squeal region, are centered around two frequencies the first one is 10000 Hz and it is labeled as region one in Fig. 11 while the other frequency is 12000 Hz which is labeled as region two. In region one it can be seen that the mode belongs to PM6 has lowest real part while the mode that belongs to PM1 has largest real part. The modes in region two the highest real part among them is that of PM2 but still all of them had low real part compared to the modes in region one. This refers to their low propensity to squeal. The tendency of instability of each configuration was calculated according to equation 7 and plotted in Fig.12 which shows that base model has the highest TOI. PM2, PM5, PM6 have nearly close values for the TOI and similarly for PM1, PM3 and PM4. PM2 has the lowest TOI of the suggested pad variations with reduction percentage 95% with respect to base model. While PM1 had highest TOI among the pad variations and the lowest reduction ratio 55% which is the lowest among the other pad shapes. It can be concluded that PM2 had the best behavior in this working condition. Figure 13 demonstrates the unstable mode generated by PM2 in the first working condition.

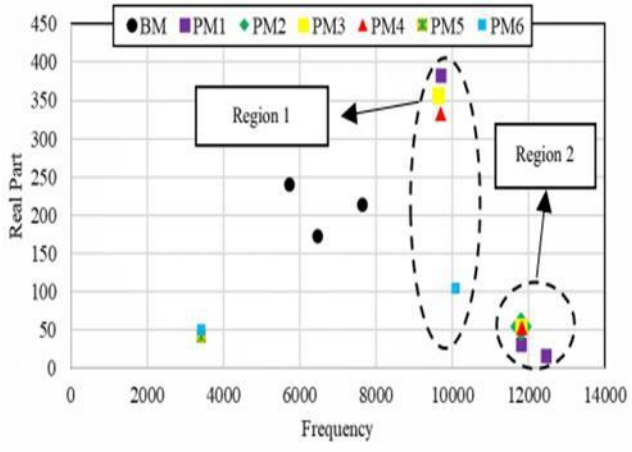

Fig. 11 The unstable modes of base model and the proposed pad modifications at the first working condition.

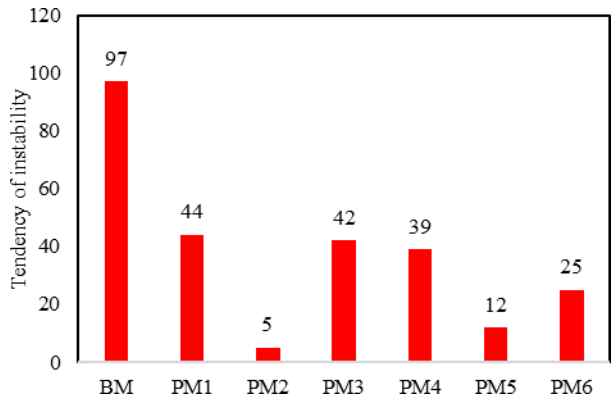

Fig. 12 The tendency of instability of each pad configuration in the first working condition.

3.2.1.2 Second working condition

In this condition the barking pressure increased from 1 to 1.5 MPa and the coefficient of friction increased from 0.45 to 0.55 causing an increase in the fiction induced instability. Consequently, it's expected that either the number of instable modes will increase or the generated modes will have high real part leads higher tendency of instability. The generated unstable modes for the base model and the proposed modifications are shown in Fig.14 and the obtained values for the frequencies, real parts are in table 5 for this case. From Fig.14 it is noticed that PM5 and PM6 generated unstable modes in the low frequency squeal region as the previous condition. In this working condition with the increase of friction the unstable modes in high frequency squeal region are centered around three main frequencies 6000, 10000 and 12000 Hz. The modes that centered around 6000 Hz are in region one in Fig.14. In region one the instable modes of the base model have the highest real pats. In region two the unstable modes are centered around 10000Hz with unstable modes that belongs to PM1 has the highest real part. In the third region the unstable modes are centered around 120000 Hz with real parts less than 100 which makes them less prone squeal. The TOI was calculated in this condition and also plotted in Fig15. Once again PM2 showed the best performance considering the increase in friction instability.PM2 lead the reduction of TOI form 107 in case of the base model to 32 with reduction percentage 70%. On the other hand, PM1 gave the least reduction percentage 25%. once again, the PM2 had the best behavior in this working state. Figure 16 displays the unstable modes of the PM2 in the second working condition.

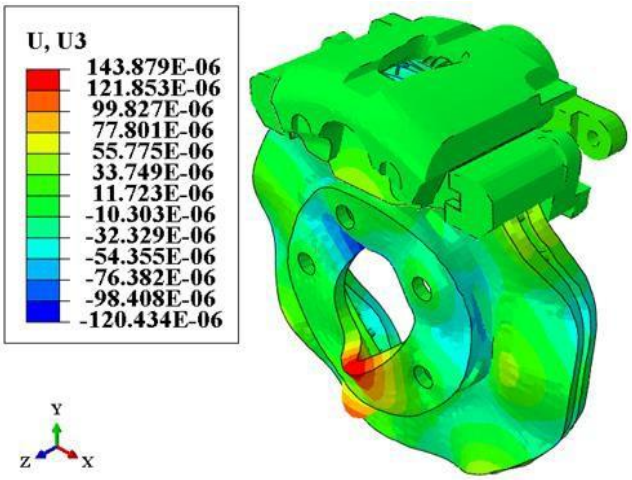

Fig. 13 The unstable mode (mode 56) of the second pad modification (PM2) at first working conditions.

Table 4 The unstable modes of the base model and each proposed pad modifications in the first working condition.

Model	Mode Number	Real Part	Frequency
BM	19	240.42	5730.11
	23	173.323	6466.82
	29	214.587	7646.23
	39	382.525	9714.51
PM1	57	30.2815	11816.3
	76	16.1073	12458.7
PM2	56	54.6411	11819.4
PM3	39	357.075	9649.81
	54	54.4037	11815.6
PM4	46	333.703	9705.68
	65	52.1775	11826.4
PM5	10	40.8532	3427.47
PM6	10	49.1506	3427.77
	43	104.464	10098

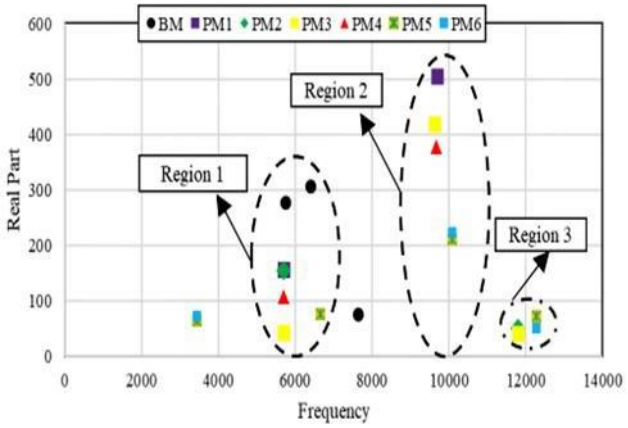

Fig. 14 The performance of base model and the proposed pad modifications at the second working condition.

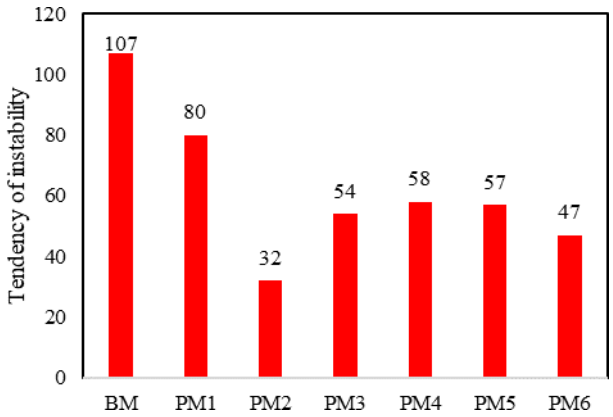

Fig. 15 The tendency of instability of each pad configuration in the second working condition.

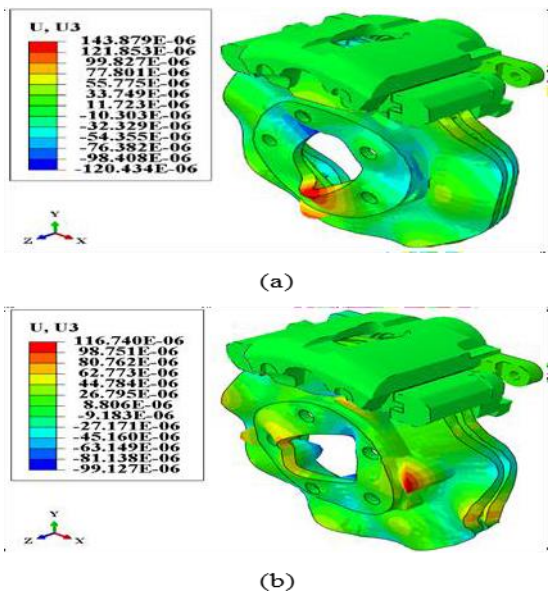

Fig. 16 The unstable modes of the PM2 in the second working condition (a) mode21 (b) mode 56.

Table 5 The unstable modes of the base model and each proposed pad modifications in the second working condition.

Model	Mode Number	Real Part	Frequency
Base Model	19	278.554	5736.8
	22	307.479	6397.73
	29	76.6743	7621.51
PM1	19	157.119	5697.61
	40	504.117	9695.94
PM2	21	153.951	5697.87
	56	51.179	11800.4
PM3	19	42.4782	5690.1
	41	418.752	9635.56
	55	40.2771	11800.1
PM4	22	107.16	5702.6
	45	377.696	9672.36
PM5	10	64.3842	3425.57
	22	75.617	6648.05
	45	211.785	10089.6
	57	72.9706	12286.1
PM6	10	71.9971	3426.16
	44	223.372	10081.2
	55	50.5796	12267.5

3.2.1.3 Third working condition

In the third working the pressure and the coefficient of friction increased causing an increase in friction induced instability. The behavior of the base model and pad modifications are shown in Fig.17 and the detailed values of frequencies and corresponding real parts are reported in table 6. In this case the base model only generated two unstable modes. All the proposed modifications generated unstable modes more the base model. PM5 and PM6 generated unstable modes in low frequency squeal region as in the previous cases. The high frequency squeal region is divided into four regions. Each region is centered around certain frequency. In the first region the center frequency is 6000 Hz. in this region PM6 has real part the base model modes. The second region has central frequency 8000 Hz however all modes in this region have real part lower 100 making them less susceptible to squeal. The third region has central frequency 10000 Hz with real part of the mode that belongs to PM1 having high value than the others. The central frequency in the fourth region is 12000 Hz but most of the modes in this region have real part less 100 except for one mode for PM2 that has real part more than 100. The TOI is plotted for the pad configurations in this case Fig.18. All the pad shapes have TOI lower than the base model except PM1 and PM6 that have higher TOI than the base model with increment percentage 20% and 21.5% for PM1 and PM6 respectively. PM3 had the lowest TOI less than base model by approximately 38% which makes it has the best behavior in this condition.

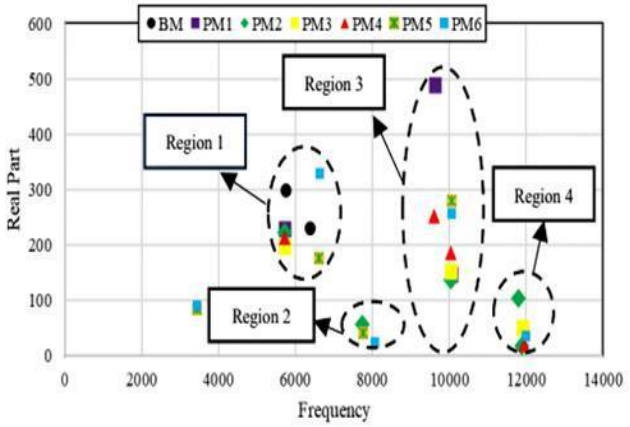

Fig. 17 The performance of base model and the proposed pad modifications at the third working condition.

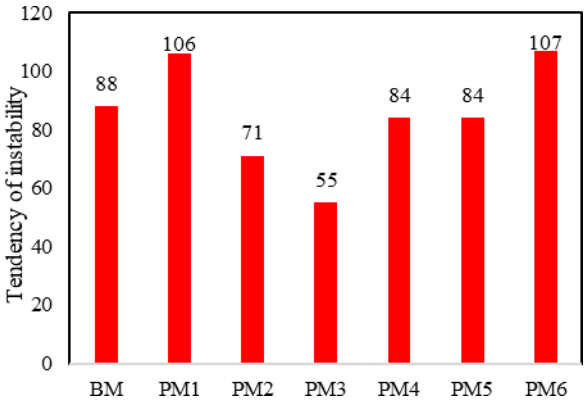

Fig. 18 The tendency of instability of each pad configuration in the third working condition.

3.2.2 Disc modifications

In that section the behavior of suggested disc modifications will be evaluated through the three various operating states. Figure 19 shows the unstable modes of each disc modification in the given conditions.

3.2.2.1 First working condition

Figure 20 illustrates the performance of the disc vanes modification and the generated modes number and values are given in table 7. The modification of disc vanes was very effective suppressing all the unstable modes of the base model compared with pad modifications in the same working conditions. The curved vane shape (DM1) has better effect than the tapered one (DM2) as the TOI is calculated and plotted in Fig.21. The TOI of the DM1 gave reduction percentage 90% compared to 53% of DM2 which indicates that DM1 performance is better in this case. Figure 22 presents the unstable mode of DM2 in the first working condition.

3.2.2.2 Second working condition

Figure 23 demonstrates the effect of disc vanes modifications in the second working conditions along with table 8 that shows the obtained values of frequencies and real parts. DM1 and DM2 showed the same behavior as in first working conditions as each one of them generated only two unstable modes. Knowing that in the second condition the friction instability is higher. In this working DM1 showed a very tendency of instability with reduction percentage 93% compared to 46% for DM2. The TOI graph for the second working conditions for the disc DM1 and DM2 is displayed in Fig.24 and Fig.25 illustrates the unstable mode of DM1 in the second working conditions.

Table 6 The unstable modes of the base model and each proposed pad modifications in the third working condition.

Model	Mode Number	Real Part	Frequency
Base Model	20	298.675	5744.64
	23	230.165	6375.43
	19	229.751	5708.03
PM1	41	489.024	9634.37
	44	147.592	10052.8
	63	5.83445	11979.7
PM2	21	223.64	5709.37
	32	57.1446	7725.12
	44	136.952	10049.5
	56	104.088	11791.3
	58	17.6964	11893.9
PM3	19	196.73	5703.17
	43	151.901	10049.3
	59	51.4925	11900.2
	62	9.6898	11932.7
PM4	24	213.969	5713.12
	47	253.162	9614.47
	50	185.863	10044.7
	70	20.3372	11956.9
PM5	10	84.8504	3422.92
	22	175.131	6613.94
	30	40.0064	7759.5
	44	279.094	10062.4
PM6	11	90.5697	3424.25
	23	328.483	6626.02
	31	23.3381	8055.3
	43	256.083	10060.2
	52	34.9536	11994.6

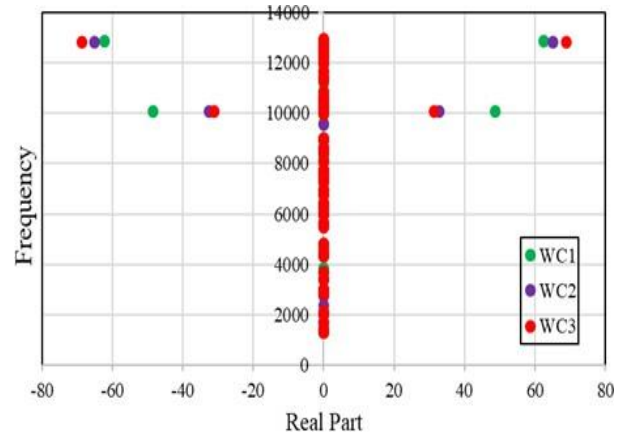

(a)

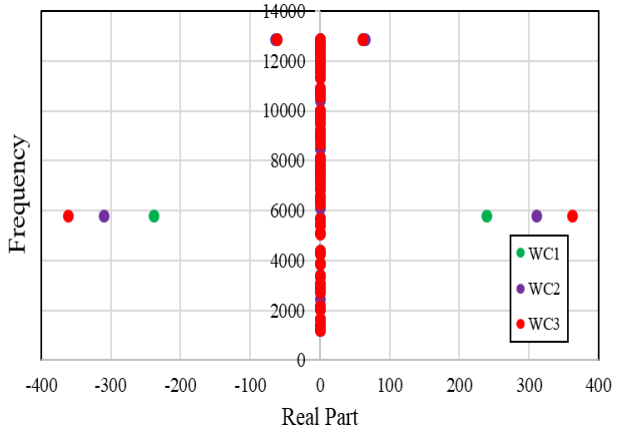

(b)

Fig. 19 The performance of each disc modification in the three given working conditions (a)DM1 (b)DM2.

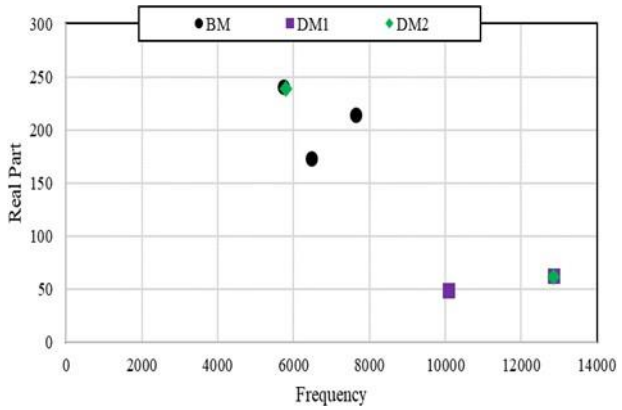

Fig. 20 The performance of base model and the proposed disc vanes modifications at the first working condition**.**

Table 7 The unstable modes of the base model and each proposed disc vanes modifications in the first working condition.

Model	Mode Number	Real Part	Frequency
Base Model	19	240.42	5730.11
	23	173.323	6466.82
	29	214.587	7646.23
DM1	40	48.6163	10087.5
	67	62.4459	12862.9
DM2	20	238.86	5804.67
	69	61.5812	12862.7

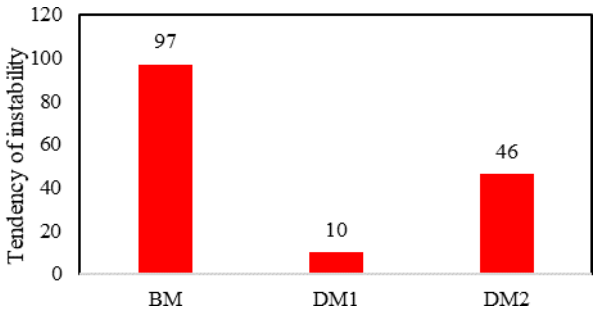

Fig. 21 The tendency of instability of each disc vanes modification in the first working condition**.**

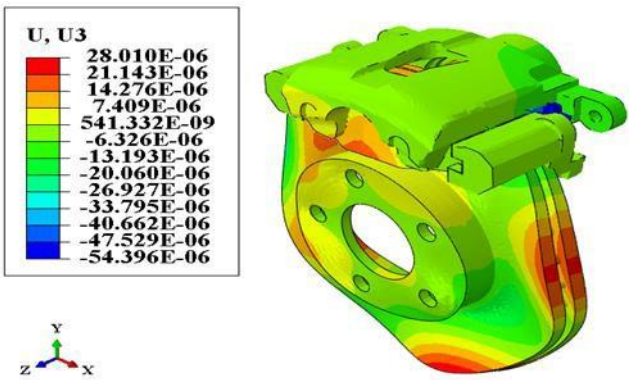

Fig. 22 The unstable mode (mode 20) of the second disc modification (DM2) in the first working conditions.

Table 8 The unstable modes of the base model and each proposed disc vanes modifications in the second working condition.

Model	Mode Number	Real Part	Frequency
Base Model	19	278.554	5736.8
	22	307.479	6397.73
	29	76.6743	7621.51
DM1	39	32.6838	10089.2
	65	65.1152	12860.2
DM2	19	310.381	5802.84
	69	64.1431	12859.8

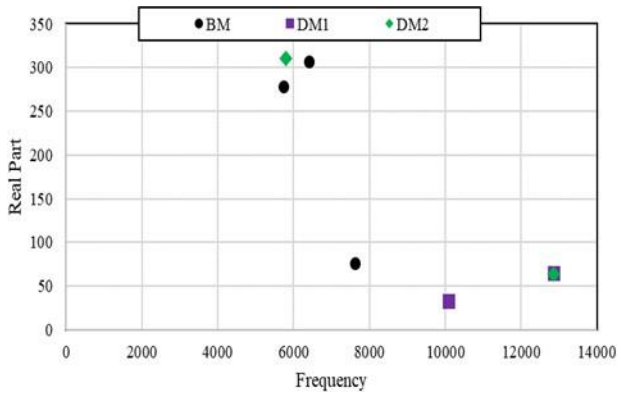

Fig. 23 The performance of base model and the proposed disc vanes modifications at the second working condition.

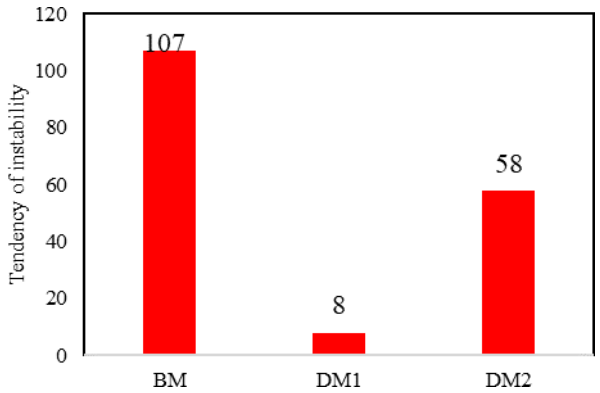

Fig.24 The tendency of instability of each disc vanes modification in the second working condition.

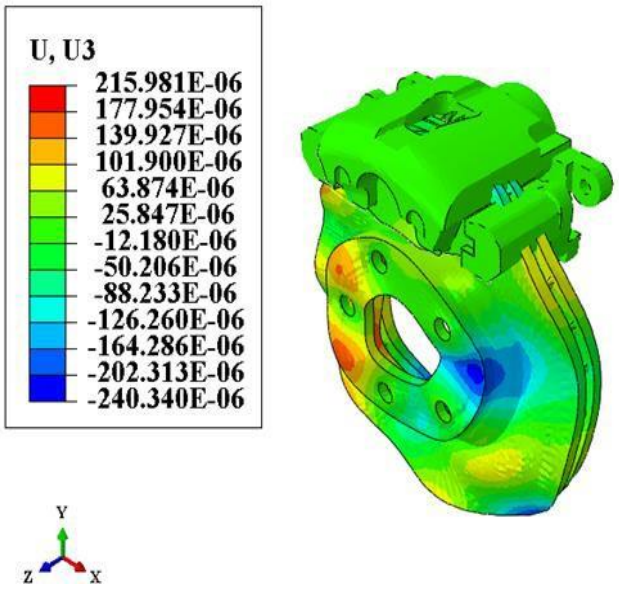

Fig. 25 The unstable mode (mode 39) of the first disc modification (DM1) in the second working conditions.

3.2.2.3 Third working condition

Figure 26 shows the performance of disc modifications in the third working condition and table 9 shows the obtained values. The performance of DM1 was better than DM2 as the TOI for DM1 in this condition was 90% less than the base model while for DM2 the reduction percentage was 24% as shown in figure 27.

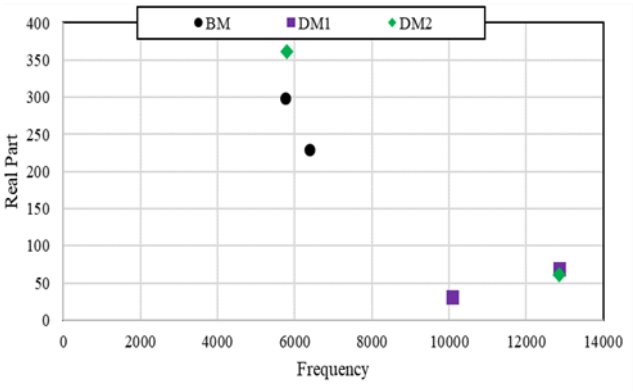

Fig.26 The performance of base model and the proposed disc vanes modifications at the third working condition.

Table 9 The unstable modes of the base model and each proposed disc vanes modification in the third working condition.

Model	Mode Number	Real Part	Frequency
Base Model	20	298.675	5744.64
	23	230.165	6375.43
DM1	39	31.3106	10087.7
	67	68.8248	12858.3
DM2	19	362.008	5803.5
	69	61.6766	12856.7

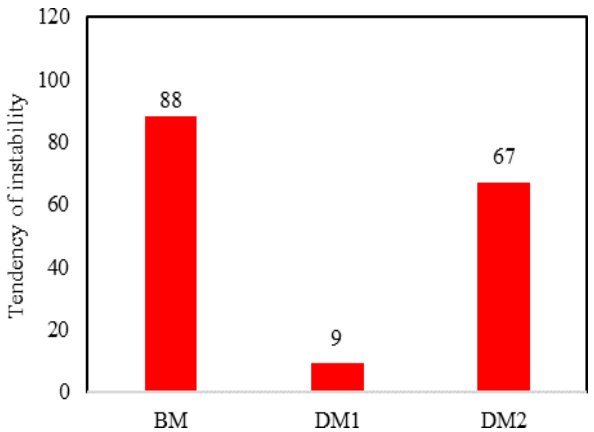

Fig.27 The tendency of instability of each disc vanes modification in the third working condition

3.3 Comparison between the pad shape and disc vanes modifications

In this section a comparison is made between the pad shape modifications and the disc vanes modifications through the given working conditions and this is done by comparing TOI values in each case. Figure 28 shows the TOI values for all pad shapes and disc vanes modifications. In the first working condition, it is noticed that PM2 is better than DM1 as it has TOI half DM1 value. Despite that DM1 performed better than all pad shape modifications. All the pad shape modifications had TOI value less than DM2. In the second working condition the situation was different, with the increase of friction as the pressure increased along with coefficient of friction the TOI value of all of disc and pad modifications increased however the TOI of DM1 decreased to 8. TOI of PM2 is four times that of DM1. For DM2 it has a close value with other pad shape modifications. so, in this case DM1 has a better performance than PM2 and all the Pad shape modifications. In the Third working condition the TOI of some pad shape modifications exceeded the base model but it is very clear that DM1 has the best behavior compared with all pad shape modifications and DM2 has lower TOI value than to all Pad shapes except for PM3.

4. Conclusion

This study describes a method for suppressing brake squeal utilizing structural changes. Six modifications of the braking pad shape along with two modifications of the disc vanes were studied through different operational conditions. Finite element analysis was carried out to evaluate the different changes of the pad and the disk. The results of the CEA and TOI showed that both pad and disc geometrical has an effect on squeal suppression however the disc modifications were more effective than that of the pad. The curved shape disc [DM1] was able to suppress all base model unstable modes of the base model with consistent manner and despite that there was another unstable mode but this mode had low tendency to squeal and with reduction percentage of TOI value of 90% for the first and third working condition and 93% for the second one than the values of the base model in the similar conditions. On the other hand, not all the pad modifications performed the same at all working conditions as despite being able to suppress some modes from the base model but another unstable mode with high tendency of squeal were generated. The results showed that the rotor modifications have high potential in squeal suppression and by carrying out design study to the rotor and determine the effective parameter either related to geometry or the material and study their effect on the brake noise generation either experimentally or numerically.

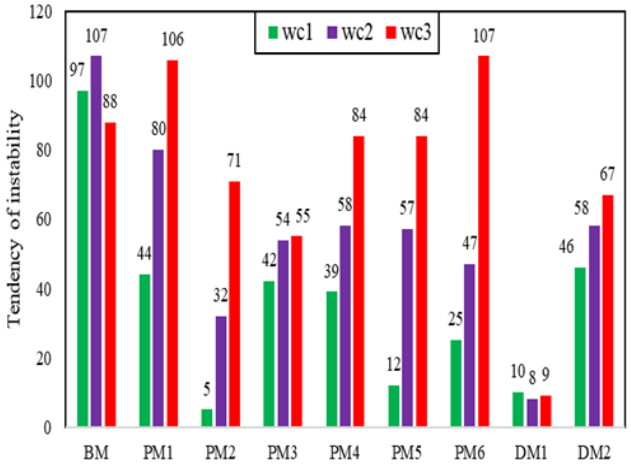

Fig. 28 The tendency of instability of pad shape and disc vanes modification in the different three working condition.

References

[1] A. Akay, "Acoustics of friction," J Acoust Soc Am, vol. 111, no. 4, pp. 1525–1548, 2002.

[2] H. Abendroth and B. Wernitz, "The integrated test concept: Dyno-vehicle, performance-noise," SAE Technical Paper, 2000.

[3] F. Chen, C. A. Tan, and R. L. Quaglia, Disc brake squeal: mechanism, analysis, evaluation, and reduction/prevention. SAE International, 2005.

[4] A. Papinniemi, J. C. S. Lai, J. Zhao, and L. Loader, "Brake squeal: a literature review," Applied acoustics, vol. 63, no. 4, pp. 391–400, 2002.

[5] N. M. Ghazaly, M. El-Sharkawy, and I. Ahmed, "A review of automotive brake squeal mechanisms," Journal of Mechanical Design and Vibration, vol. 1, no. 1, pp. 5–9, 2014.

[6] H. Sujay and B. S. Suresh, "Study of Friction Induced Stick-Slip Phenomenon in a Minimal Disc Brake Model," Journal of Mechanical Engineering and Automation, vol. 5, no. B, 2015.

[7] H. R. Mills, "Brake squeal. Institution of automobile engineers," Report, 1938.

[8] R. T. Spurr, "A theory of brake squeal," Proceedings of the Institution of Mechanical Engineers: Automobile Division, vol. 15, no. 1, pp. 33–52, 1961.

[9] M. R. North, Disc brake squeal-a theoretical model. MIRA, 1972.

[10] M. R. North, "Disc brake squeal. Braking of Road Vehicles, Automobile Division of the Institution of Mechanical Engineers." Mechanical Engineering Publications Limited, London, England, 1976.

[11] S. K. Rhee, P. H. S. Tsang, and Y. S. Wang, "Friction-induced noise and vibration of disc brakes," Wear, vol. 133, no. 1, pp. 39–45, 1989.

[12] D. Zhu et al., "Noise and vibration performance of automotive disk brakes with laser-machined M-shaped grooves," Proceedings of the Institution of Mechanical Engineers, Part D: Journal of Automobile Engineering, vol. 237, no. 5, 2023, doi: 10.1177/09544070221085972.

[13] N. Singla, J.-F. Brunel, A. Mège-Revil, H. Kasem, and Y. Desplanques, "Experiment to investigate the relationship between the third-body layer and the occurrence of squeals in dry sliding contact," Tribol Lett, vol. 68, pp. 1–11, 2020.

[14] M. Triches Jr, S. N. Y. Gerges, and R. Jordan, "Reduction of squeal noise from disc brake systems using constrained layer damping," Journal of the Brazilian Society of Mechanical Sciences and Engineering, vol. 26, pp. 340–348, 2004.
[15] U. von Wagner, D. Hochlenert, and P. Hagedorn, "Minimal models for disk brake squeal," J Sound Vib, vol. 302, no. 3, pp. 527–539, 2007.
[16] C. Cantoni, R. Cesarini, G. Mastinu, G. Rocca, and R. Sicigliano, "Brake comfort–a review," Vehicle System Dynamics, vol. 47, no. 8, pp. 901–947, 2009.
[17] N. M. Kinkaid, O. M. O'Reilly, and P. Papadopoulos, "Automotive disc brake squeal," J Sound Vib, vol. 267, no. 1, pp. 105–166, 2003.
[18] D. Wei, J. Song, Y. Nan, and W. Zhu, "Analysis of the stick-slip vibration of a new brake pad with double-layer structure in automobile brake system," Mech Syst Signal Process, vol. 118, 2019, doi: 10.1016/j.ymssp.2018.08.055.
[19] P. K. Sahoo and S. Chatterjee, "Effect of high-frequency excitation on friction induced vibration caused by the combined action of velocity-weakening and mode-coupling," Journal of Vibration and Control, vol. 26, no. 9–10, pp. 735–746, 2020.
[20] D. Wang, R. Wang, T. Heng, G. Xie, and D. Zhang, "Tribo-brake characteristics between brake disc and brake shoe during emergency braking of deep coal mine hoist with the high speed and heavy load," Energies (Basel), vol. 13, no. 19, p. 5094, 2020.
[21] N. Liu and H. Ouyang, "Friction-induced vibration considering multiple types of nonlinearities," Nonlinear Dyn, vol. 102, pp. 2057–2075, 2020.
[22] A. Ghorbel, B. Zghal, M. Abdennadher, L. Walha, and M. Haddar, "A new approach considering the brake pad geometry in brake squeal," Archive of Applied Mechanics, vol. 89, pp. 2075–2088, 2019.
[23] H. Ouyang, W. Nack, Y. Yuan, and F. Chen, "Numerical analysis of automotive disc brake squeal: a review," International Journal of Vehicle Noise and Vibration, vol. 1, no. 3–4, 2005, doi: 10.1504/ijvnv.2005.007524.
[24] W. V Nack and A. M. Joshi, "Friction induced vibration: brake moan," SAE transactions, pp. 1967–1973, 1995.
[25] G. Ostermeyer, "Dynamic friction laws and their impact on friction induced vibrations," SAE Technical Paper, 2010.
[26] G. D. Liles, "Analysis of disc brake squeal using finite element methods," SAE transactions, pp. 1138–1146, 1989.
[27] A. Bajer, V. Belsky, and L. J. Zeng, "Combining a nonlinear static analysis and complex eigenvalue extraction in brake squeal simulation," SAE technical paper, 2003.
[28] N. Coudeyras, S. Nacivet, and J.-J. Sinou, "Periodic and quasi-periodic solutions for multi-instabilities involved in brake squeal," J Sound Vib, vol. 328, no. 4–5, pp. 520–540, 2009.
[29] A. R. AbuBakar and H. Ouyang, "Complex eigenvalue analysis and dynamic transient analysis in predicting disc brake squeal," International Journal of Vehicle Noise and Vibration, vol. 2, no. 2, pp. 143–155, 2006.
[30] W. Liu and J. Pfeifer, "Reducing high frequency disc brake squeal by pad shape optimization," SAE transactions, pp. 572–576, 2000.
[31] J. D. Fieldhouse, W. P. Steel, C. J. Talbot, and M. A. Siddiqui, "Rotor asymmetry used to reduce disc brake noise," SAE Technical Paper, 2004.
[32] M. N. M. Nouby and K. S. K. Srinivasan, "Parametric studies of disc brake squeal using finite element approach," Jurnal Mekanikal, 2009.
[33] M. Nouby, C. Sujatha, and K. Srinivasan, "Modelling of automotive disc brake squeal and its reduction using rotor design modifications," International Journal of Vehicle Noise and Vibration, vol. 7, no. 2, pp. 129–148, 2011.
[34] C. Kim and K. Zhou, "Analysis of automotive disc brake squeal considering damping and design modifications for pads and a disc," International Journal of Automotive Technology, vol. 17, pp. 213–223, 2016.
[35] T. Jung, Y. Hong, S. Park, C. Kim, Y. Hong, and C. Cho, "Numerical study for brake squeal by machining patterns on frictional surface," International Journal of Automotive Technology, vol. 19, pp. 281–289, 2018.
[36] G. Pan, X. Zhang, P. Liu, and L. Chen, "Impact analysis of contact symmetrical caliper structure on brake squeal," JVC/Journal of Vibration and Control, vol. 27, no. 19–20. 2021. doi: 10.1177/1077546320959517.
[37] C. Kim, Y. Kwon, and D. Kim, "Analysis of low-frequency squeal in automotive disc brake by optimizing groove and caliper shapes," International Journal of Precision Engineering and Manufacturing, vol. 19, pp. 505–512, 2018.
[38] Y. Gu, Y. Liu, C. Lu, S. Hu, and X. Song, "Effect of compressive strain of brake pads on brake noise," Shock and Vibration, vol. 2020, pp. 1–11, 2020.
[39] O. I. Abdullah, N. Stojanovic, and I. Grujic, "The Influence of the Braking Disc Ribs and Applied Material on the Natural Frequency," International Journal of Precision Engineering and Manufacturing, pp. 1–11, 2022.
[40] Z. Y. Xiang, W. Chen, J. L. Mo, Q. A. Liu, Z. Y. Fan, and Z. R. Zhou, "The effects of the friction block shape on the tribological and dynamical behaviors of high-speed train brakes," Int J Mech Sci, vol. 194, p. 106184, 2021.
[41] S. Yang, Z. Sun, Y. Liu, B. Lu, T. Liu, and H. Hou, "Automotive brake squeal simulation and optimization," SAE International Journal of Passenger Cars-Mechanical Systems, vol. 9, no. 2016-01–1298, pp. 174–182, 2016.
[42] G. Dihua and J. Dongying, "A study on disc brake squeal using finite element methods," in SAE Technical Papers, 1998. doi: 10.4271/980597.
[43] Y. K. Wu, B. Tang, Z. Y. Xiang, H. H. Qian, J. L. Mo, and Z. R. Zhou, "Brake squeal of a high-speed train for different friction block configurations," Applied Acoustics, vol. 171, 2021, doi: 10.1016/j.apacoust.2020.107540.
[44] Q. Zhu, G. X. Chen, B. W. Wu, and X. Kang, "Effect of the Material Parameter and Shape of Brake Pads on Friction-Induced Disc Brake Squeal of a Railway Vehicle," Tribology Transactions, vol. 64, no. 4, 2021, doi: 10.1080/10402004.2021.1914254.
[45] G. S. Chen and X. Liu, Friction Dynamics: Principles and Applications. 2016.
[46] M. Nouby and K. Srinivasan, "Simulation of the structural modifications of a disc brake system to reduce brake squeal," in Proceedings of the Institution of Mechanical Engineers, Part D: Journal of Automobile Engineering, 2011. doi: 10.1177/2041299110394515.